Journal of Organometallic Chemistry 875 (2018) 35–45

Contents lists available at ScienceDirect

Journal of Organometallic Chemistry

journal homepage: www.elsevier.com/locate/jorganchem

A highly efficient heterogeneous palladium-catalyzed carbonylative annulation of 2-aminobenzamides with aryl iodides leading to quinazolinones

Shengyong You [a, b], Bin Huang [a], Tao Yan [a], Mingzhong Cai [a, *]

[a] Key Laboratory of Functional Small Organic Molecule, Ministry of Education and College of Chemistry & Chemical Engineering, Jiangxi Normal University, Nanchang, 330022, PR China
[b] Institute of Applied Chemistry, Jiangxi Academy of Sciences, Nanchang, 330029, PR China

ARTICLE INFO

Article history:
Received 25 May 2018
Received in revised form
14 August 2018
Accepted 1 September 2018
Available online 4 September 2018

Keywords:
Carbonylative annulation
Palladium
Quinazolinone
2-Aminobenzamide
Heterogeneous catalysis

ABSTRACT

The first heterogeneous carbonylative annulation of 2-aminobenzamides with aryl iodides was achieved in *N,N*-dimethylformamide (DMF) at 120 °C under 10 bar of carbon monoxide by using an MCM-41-immobilized bidentate phosphine palladium(II) complex [MCM-41-2P-Pd(OAc)$_2$] as catalyst and 1,8-diazabicycloundec-7-ene (DBU) as base, yielding a wide variety of quinazolinone derivatives in good to excellent yields. The new heterogeneous palladium catalyst can easily be prepared by a simple procedure from commercially readily available reagents, and recovered by filtration of the reaction solution, and recycled up to eight times without significant loss of activity.

1. Introduction

Quinazolinones, existing in many natural alkaloids and pharmaceuticals [1,2], are a significant class of annulated six-membered nitrogen heterocycles. They are endowed with numerous pharmacological and biological activities, including anticancer [3,4], antibacterial [5], antifungal [6], antimalarial [7], antihypertensive [8], antitubercular [9], inhibitors of derived growth factor receptor phosphorylation [10], anticonvulsant [11], and other activities [12–14]. Additionally, quinazolinones are also important building blocks in the synthesis of natural products and bioactive compounds [15,16]. As a result, a number of methods have been developed for construction of quinazolinones [17]. Conventionally, such a structure is synthesized by the condensation of 2-halobenzoic acids, 2-halobenzamides, 2-aminobenzamides, 2-aminobenzoic acids with amidines, benzyl alcohols, benzylamines, acid amides or amino acids [18–21]. However, these known methods generally suffer from certain disadvantages, such as multistep synthesis, low yields, limited substrate scope, and/or harsh reaction conditions. These problems have stimulated several groups to apply transition metal-catalyzed reactions for the development of new protocols to substituted quinazolinones, using Cu [22], Ir [23], Pt [24], and Pd [25–27] as catalysts.

Since the pioneering work of Heck and co-workers in 1974 [28], palladium-catalyzed carbonylative transformation of organohalides has become a powerful tool in modern organic synthesis [29–31]. The advantages of carbonylation reactions are (i) it is the most potent methodology in the construction of carbonyl-containing compounds, which increases the carbon number at the same time, and (ii) carbon monoxide (CO) can be used as a cheap and readily available C1 source, which is also in agreement with the green chemistry principles. Recently, palladium-catalyzed carbonylative annulation reactions have been successfully applied in the synthesis of furanones, benzoxazinones, flavones, and other heterocycles [32–35]. Wu and coworkers reported a palladium-catalyzed carbonylative synthesis of quinazolinones from 2-aminobenzamide and aryl bromides with expensive BuPAd$_2$ (di-1-adamantyl-*n*-butylphosphine) as the ligand [36] [Eq. (1), in Scheme 1]. Although these palladium-catalyzed carbonylative annulation reactions are highly efficient for the construction of heterocycles, industrial applications of these homogeneous palladium complexes remain a challenge because they are quite expensive, cannot be recycled, and difficult to

* Corresponding author.
E-mail addresses: caimzhong@163.com, mzcai@jxnu.edu.cn (M. Cai).

https://doi.org/10.1016/j.jorganchem.2018.09.003
0022-328X/

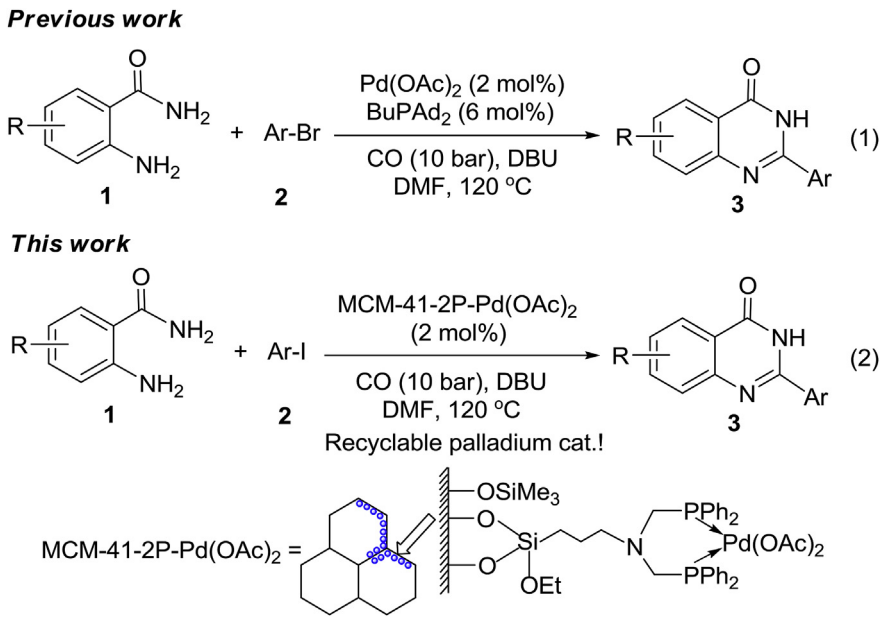

Scheme 1. Palladium-catalyzed carbonylative synthesis of quinazolinones.

separate from the product mixture, which is a particularly significant drawback for their applications in the pharmaceutical industry. Immobilization of the existing homogeneous palladium catalysts on porous materials with high surface areas could be an attractive solution to these problems since the immobilized catalysts can be facilely separated from the reaction mixture by a simple filtration process, and recycled for several times. There has been considerable interest in the development of heterogeneous palladium catalytic systems that can be efficiently recycled whilst maintaining the inherent activity of the catalytic centre [37].

Mesoporous MCM-41 materials have recently been shown to be powerful supports for immobilization of homogeneous catalysts due to their outstanding advantages, such as extremely high surface areas, large and defined pore sizes, big pore volumes and the presence of a large number of silanol (Si—OH) groups on the inner surface in comparison with other solid supports [38–40]. So far, some palladium [41–44], rhodium [45], molybdenum [46], gold [47–49] and copper [50–52] complexes immobilized on MCM-41 have been successfully used as highly active and recyclable catalysts in organic reactions. As a part of our continuing interest in the development of efficient heterogeneous catalysts for organic synthesis [43,49–52], herein we report the synthesis of an MCM-41-immobilized bidentate phosphine palladium(II) complex [MCM-41-2P-Pd($OAc)_2$] and its successful application to carbonylative annulation of 2-aminobenzamides with aryl iodides under 10 bar of CO leading to a wide variety of 2-aryl-substituted quinazolinones in good to excellent yields [Eq. (2), in Scheme 1]. The new heterogeneous palladium catalyst exhibits high catalytic activity in the reaction and can be facilely recovered *via* a simple filtration process after the reactions, and its catalytic efficiency remains unchanged even after recycling eight times.

2. Results and discussion

2.1. Synthesis and characterization of MCM-41-2P-Pd($OAc)_2$ complex

The MCM-41-immobilized bidentate phosphine palladium(II) complex [MCM-41-2P-Pd($OAc)_2$] was synthesized starting from mesoporous material MCM-41, *N,N*-bis((diphenylphosphino) methyl)-3-(triethoxysilyl)propan-1-amine, and $Pd(OAc)_2$ according to the procedure summarized in Scheme 2. Firstly, the condensation of *N,N*-bis((diphenylphosphino)methyl)-3-(triethoxysilyl) propan-1-amine with MCM-41 in toluene at 100 °C for 24 h, followed by the silylation with Me_3SiCl in toluene at room temperature for 24 h gave a bidentate phosphino-functionalized MCM-41 material (MCM-41-2P). The latter was subsequently reacted with $Pd(OAc)_2$ in acetone under reflux for 72 h to generate the MCM-41-immobilized bidentate phosphine palladium(II) complex [MCM-41-2P-Pd($OAc)_2$] as a light yellow powder. The palladium content of this complex was determined to be 0.36 mmol/g (3.83 wt%) by ICP-AES. The energy dispersive X-ray spectroscopy (EDS) shows the elements present in the material. EDS analysis of fresh MCM-41-2P-Pd($OAc)_2$ complex (Fig. 1) shows the presence of Si, O, C, N, P, and Pd elements, confirming the successful anchoring of the palladium-phosphine complex onto the MCM-41. The silanization of MCM-41 was further confirmed by FTIR spectroscopy (Fig. 2). The FTIR spectrum (Fig. 2a) of MCM-41 shows the Si—O stretching absorption around 1095 cm^{-1}. In the FTIR spectrum (Fig. 2b) of MCM-41-2P-Pd($OAc)_2$ absorptions at 1630, 1572 and 1413 cm^{-1} (benzene ring) were observed, indicating the presence of silylated palladium(II)- phosphine groups.

Fig. 3 shows the XRD patterns for the parent MCM-41 and the MCM-41-2P-Pd($OAc)_2$ complex. Small angle X-ray diffraction pattern of the parent MCM-41 showed three peaks corresponding to hexagonally ordered mesoporous phases. For the MCM-41-2P-Pd($OAc)_2$, the (100) reflection of the parent MCM-41 was maintained after introduction of the palladium complex, but the intensity decreased apparently, while the (110) and (200) reflections became weak and diffuse, which may be mainly due to contrast matching between the silicate framework and organic moieties which are located inside the channels of MCM-41. These results indicate that the structure of the mesoporous MCM-41 remains intact through the functionalization procedure, and the formation of the catalyst has taken place preferentially inside the pore system of MCM-41.

Morphological changes of MCM-41 and MCM-41-2P-Pd($OAc)_2$ were investigated by scanning electron microscopy (SEM). As shown in Fig. 4, the morphology of MCM-41-2P-Pd($OAc)_2$ (Fig. 4b

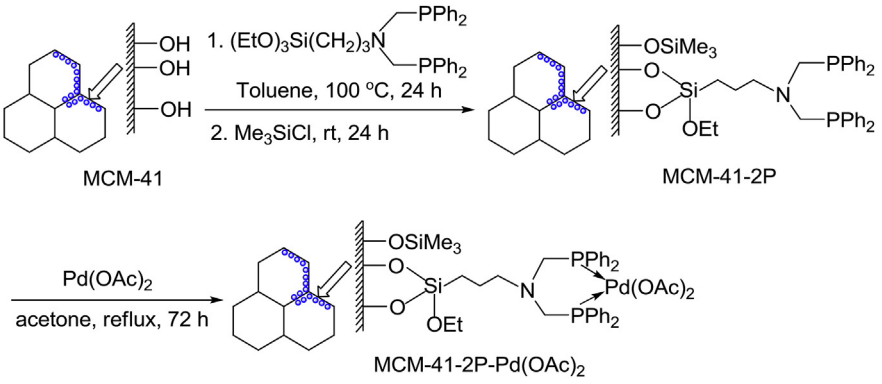

Scheme 2. Preparation of MCM-41-2P-Pd(OAc)$_2$ complex.

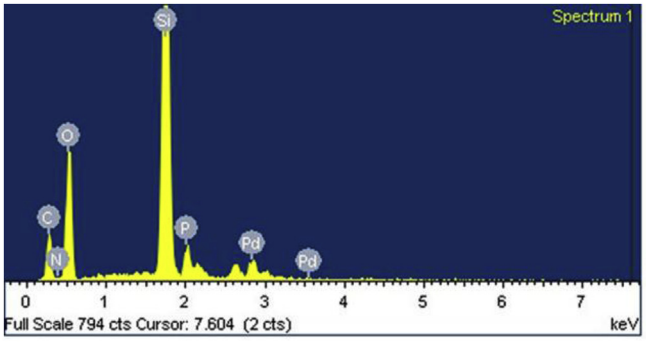

Fig. 1. Energy dispersive spectra (EDS) of MCM-41-2P-Pd(OAc)$_2$.

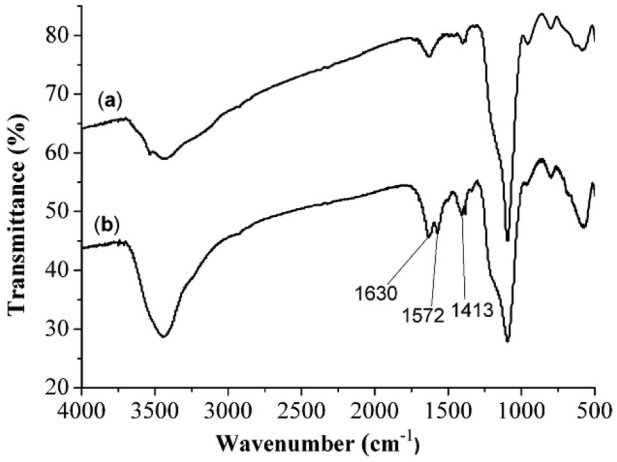

Fig. 2. FTIR spectra of MCM-41 (a) and MCM-41-2P-Pd(OAc)$_2$ (b).

and d) is similar to the particle form of MCM-41 (Fig. 4a and c), suggesting a high possibility in the modification of palladium complex on the inner channel of MCM-41 pores without any significant change in the manner of MCM-41. The N_2 adsorption-desorption isotherms and pore size distributions for MCM-41 and MCM-41-2P-Pd(OAc)$_2$ are illustrated in Fig. 5 and Fig. 6, respectively. As expected, the isotherms in Fig. 5 have remarkable changes before and after grafting because the organic moieties entered the channels, but both samples showed type IV isotherms, characteristic of mesoporous materials according to the IUPAC classification. As presented in Fig. 6, the pore volume and size of MCM-41-2P-Pd(OAc)$_2$ decreased apparently, compared with MCM-41, also

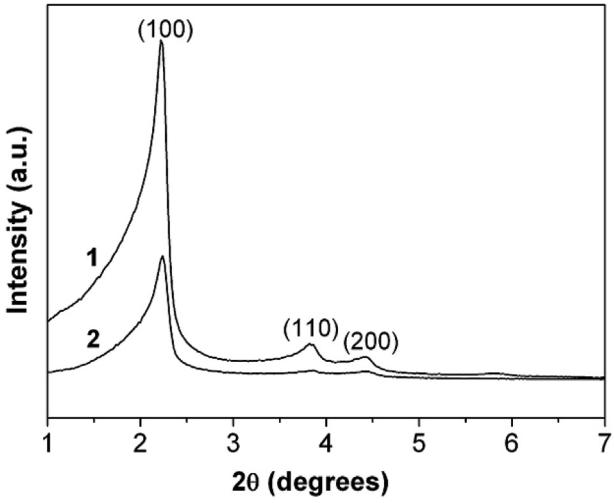

Fig. 3. XRD patterns of the parent MCM-41 (**1**) and MCM-41-2P-Pd(OAc)$_2$ (**2**).

indicating that the organic moieties were introduced into the inner channels, but the pore still remained a narrow distribution. After grafting the bidentate phosphine-palladium complex onto MCM-41, the surface area and pore diameter decreased from 967.3 m^2/g and 2.7 nm to 658.4 m^2/g and 2.3 nm, respectively, indicating that the ordered mesostructure of the parent MCM-41 remained almost unaltered. XPS analysis of the fresh MCM-41-2P-Pd(OAc)$_2$ complex was also performed to analyze the oxidation state of the Pd metal (Fig. 7a). The observed binding energy values of 342.6 eV (Pd $3d^{3/2}$) and 337.3 eV (Pd $3d^{5/2}$) on the XPS spectrum of the catalyst indicated the existence of palladium as Pd(II) form.

2.2. Heterogeneous palladium-catalyzed carbonylative annulation of 2-aminobenzamides with aryl iodides

The MCM-41-immobilized bidentate phosphine palladium(II) complex [MCM-41-2P-Pd(OAc)$_2$] was then used as catalyst for carbonylative annulation of 2-aminobenzamides with aryl iodides. Initial experiments, with 2-aminobenzamide (**1a**) and iodobenzene (**2a**) under 10 bar of carbon monoxide, were performed to optimize the reaction conditions (base, solvent, reaction temperature, catalyst quantity), and the results are summarized in Table 1. At first, the base effect was examined in the presence of 2 mol% of MCM-41-2P-Pd(OAc)$_2$ in DMF as solvent at 120 °C, and a significant base effect was observed. When DIPEA (diisopropylethylamine), *n*-Bu_3N, DMAP (4-dimethylaminopyridine), and

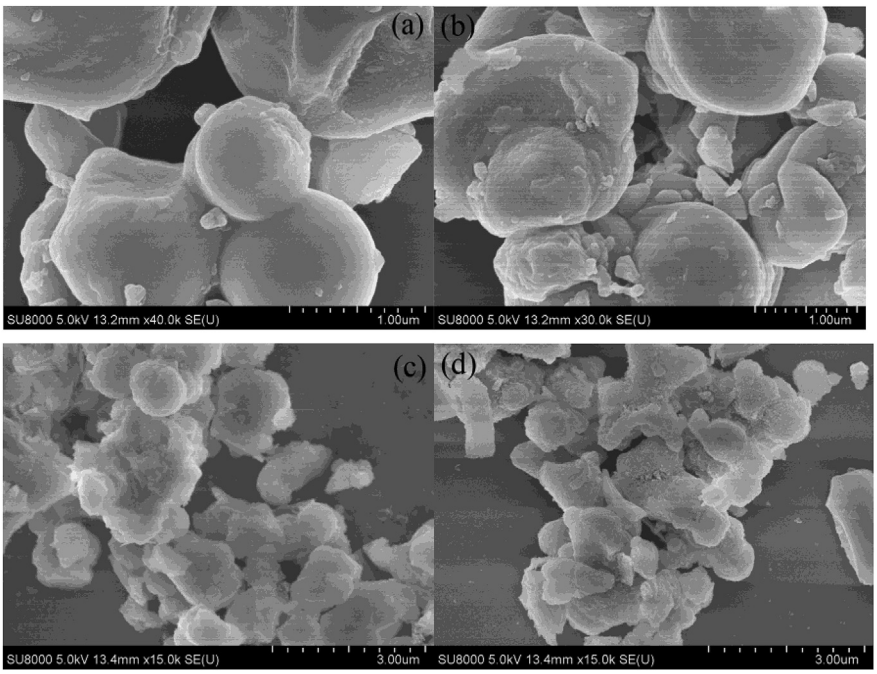

Fig. 4. SEM images of MCM-41 (a and c) and MCM-41-2P-Pd(OAc)$_2$ (b and d).

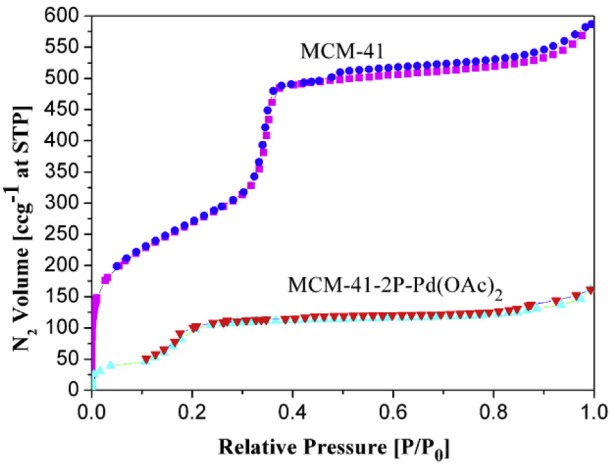

Fig. 5. N_2 adsorption/desorption isotherms of MCM-41 and MCM-41-2P-Pd(OAc)$_2$.

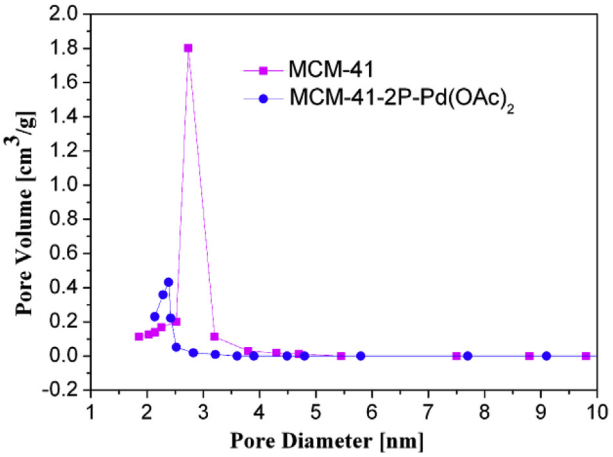

Fig. 6. Pore size distributions of MCM-41 and MCM-41-2P-Pd(OAc)$_2$.

DABCO(1,4-diazabicyclo [2,2,2]octane) were used as bases, the reaction produced 2-phenylquinazolin-4(*3H*)-one (**3a**) in low yields (entries 1–4). To our delight, the yield of the desired **3a** can be improved to 90% by using DBU (1,8-diazabicyclo[5,4,0]undec-7-ene) as base (entry 5), whereas inorganic bases such as K_2CO_3 and Cs_2CO_3 were ineffective (entries 6 and 7). Our next studies focused on the effect of solvent on the model reaction by using DBU as base (entries 8–11). When DMAc was used as solvent, the desired **3a** was also isolated in high yield, while other solvents such as NMP, DMSO and DMI were substantially less effective. So, DMF was the best choice (entry 5). Lowering reaction temperature resulted in a decreased yield, and a considerable amount of non-cyclized amide [*N*-(2-carbamoylphenyl)benzamide] was detected as the by-product (entries 12 and 13). Raising reaction temperature to 130 °C also resulted in a slightly decreased yield (entry 14). When Pd(OAc)$_2$ (2 mol%) and DPPP [1,3-bis(diphenylphosphino) propane] (3 mol%) were used as catalyst system, the desired product **3a** was isolated in 91% yield (entry 15), indicating that the catalytic activity of the MCM-41-2P-Pd(OAc)$_2$ complex was comparable to that of homogeneous Pd(OAc)$_2$/DPPP system. The use of commercially available catalysts such as $PdCl_2(PPh_3)_2$ or Pd/C resulted in a low yield or no formation of the desired product (entries 16 and 17), which revealing the key role of the ligand in this transformation. Reducing the amount of the catalyst to 1 mol% resulted in a lower yield, and a long reaction time was required (entry 18). Increasing the amount of the catalyst to 4 mol% could shorten the reaction time, but did not improve the yield significantly (entry 19). In order to check the effect of Pd loading of the catalyst on the reaction, the MCM-41-2P-Pd(OAc)$_2$ complexes with different Pd loadings were prepared by varying the MCM-41-2P/Pd(OAc)$_2$ feed ratio. The use of MCM-41-2P-Pd(OAc)$_2$ with Pd loading of 2.15 wt% resulted in a significant decrease in the yield, and MCM-41-2P-Pd(OAc)$_2$ with Pd loading of 4.94 wt% also afforded a relatively lower yield (entries 20 and 21). So, the MCM-41-2P-Pd(OAc)$_2$ complex with Pd loading of 3.83 wt% was the most efficient for this transformation. Thus, the optimized reaction conditions for this carbonylative annulation are the use of MCM-41-2P-

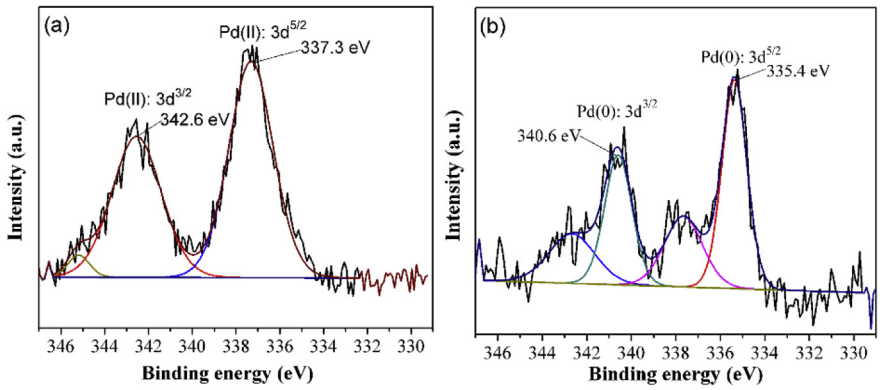

Fig. 7. XPS of the fresh MCM-41-2P-Pd(OAc)$_2$ (a) and recycled MCM-41-2P-Pd(OAc)$_2$ (b).

Table 1
Carbonylative annulation of 2-aminobenzamide with iodobenzene in different conditions.[a]

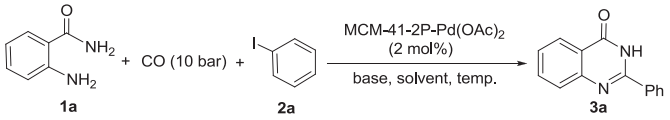

1a 2a 3a

Entry	Base	Solvent	Temp. (°C)	Time (h)	Yield (%)[b]
1	DIPEA	DMF	120	24	15
2	*n*-Bu$_3$N	DMF	120	24	21
3	DMAP	DMF	120	24	29
4	DABCO	DMF	120	24	37
5	DBU	DMF	120	20	90
6	K_2CO_3	DMF	120	24	trace
7	Cs_2CO_3	DMF	120	24	trace
8	DBU	DMAc	120	20	87
9	DBU	NMP	120	24	63
10	DBU	DMSO	120	24	54
11	DBU	DMI	120	24	48
12	DBU	DMF	110	24	78
13	DBU	DMF	100	24	32
14	DBU	DMF	130	20	87
15[c]	DBU	DMF	120	20	91
16[d]	DBU	DMF	120	24	46
17[e]	DBU	DMF	120	24	0
18[f]	DBU	DMF	120	40	69
19[g]	DBU	DMF	120	12	91
20[h]	DBU	DMF	120	24	67
21[i]	DBU	DMF	120	24	84

[a] Reaction conditions: **1a** (1 mmol), **2a** (1 mmol), base (2 mmol), MCM-41-2P-Pd(OAc)$_2$ (2 mol%) in solvent (2 mL) under 10 bar of CO.
[b] Isolated yield.
[c] Pd(OAc)$_2$ (2 mol%) and DPPP (3 mol%) were used.
[d] $PdCl_2(PPh_3)_2$ (2 mol%) was used.
[e] Pd/C (2 mol%) was used.
[f] MCM-41-2P-Pd(OAc)$_2$ (1 mol%) was used.
[g] MCM-41-2P-Pd(OAc)$_2$ (4 mol%) was used.
[h] MCM-41-2P-Pd(OAc)$_2$ with Pd loading of 2.15 wt% (2 mol%) was used.
[i] MCM-41-2P-Pd(OAc)$_2$ with Pd loading of 4.94 wt% (2 mol%) was used.

Pd(OAc)$_2$ (2 mol%), DBU (2 equiv.) as base in DMF as solvent at 120 °C under 10 bar of CO for 20 h (Table 1, entry 5).

With the optimized reaction conditions in hand, the generality of this convenient and practical methodology was tested by using various 2-aminobenzamides and a variety of aryl iodides as substrates, and the results are listed in Table 2. First, the scope of aryl iodides was examined by using 2-aminobenzamide (**1a**) as substrate. As shown in Table 2, both electron-rich and electron-deficient aryl iodides could undergo the carbonylative annulation with 2-aminobenzamide (**1a**) effectively under identical conditions to afford the corresponding 2-arylquinazolinones **3b-3i** in 60–85% yields. The reactivity of aryl iodides bearing electron-withdrawing groups was lower than that of aryl iodides having electron-donating groups. For example, the reactions of aryl iodides having strong electron-withdrawing groups such as 4-(trifluoromethyl) iodobenzene (**2g**), 4-iodobenzonitrile (**2h**), and 4′-iodoacetophenone (**2i**) gave the corresponding products **3g-3i** in only 60–65% yields. The sterically hindered 2-iodoanisole (**2j**) and 2-chloroiodobenzene (**2k**) also afforded the expected quinazolinones **3j** and **3k** in good yields. Bulky 1-iodonaphthalene (**2l**) can be applied as substrate as well and gave the desired 2-(naphthalen-1-yl)quinazolin-4(*3H*)-one (**3l**) in 91% yield. Heteroatoms turned out to be compatible with the employed reaction conditions. The reactions of 2-iodofuran (**2m**), 2-iodothiophene (**2n**), 4-iodopyridine (**2o**), and 3-iodopyridine (**2p**) with **1a** could give the corresponding 2-heterocycle substituted quinazolinones **3m-3p** in good yields.

The optimized reaction conditions were also applied to the carbonylative annulation of substituted 2-aminobenzamides with a variety of aryl and heteroaryl iodides, the results are also listed in Table 2. 2-Aminobenzamides bearing various substituents **1b-1f**, regardless of their electronic properties and substitution positions, could undergo the carbonylative annulation with various aryl or heteroaryl iodides smoothly to give a variety of quinazolinone derivatives **3q-3e'** in 62–90% yields. The reactivity of electron-rich 2-aminobenzamides was higher than that of electron-deficient ones. In addition, three examples of biologically active analogues **3f'-3h'** (Acetildenafil and Sildenafil) were prepared by this methodology in good yields through the reaction of 4-amino-1-methyl-3-*n*-propyl-5-pyrazolecarboxamide (**1g**) with aryl iodides. A wide range of functional groups, such as methyl, methoxy, chloro, fluoro, trifluoromethyl, cyano, acetyl, and nitro were tolerated well. The present method provides a novel, efficient and practical procedure for the preparation of a variety of quinazolinone derivatives. Remarkably, all of the products described here were purified by simple filtration or recrystallization and no chromatography was needed, which indicating the suitability of this protocol for large scale application.

2.3. Leaching test for MCM-41-2P-Pd(OAc)$_2$

It would be a concern if the leaching of active Pd species into the solution is substantial. A hot-filtration experiment [53] was performed to examine the leaching of palladium species from MCM-41-2P-Pd(OAc)$_2$. For this, the carbonylative annulation reaction of 2-aminobenzamide (**1a**) with iodobenzene (**2a**) was carried out until a conversion of approximately 30%. Then the catalyst was

Table 2
Heterogeneous palladium-catalyzed carbonylative synthesis of quinazolinones.[a,b]3

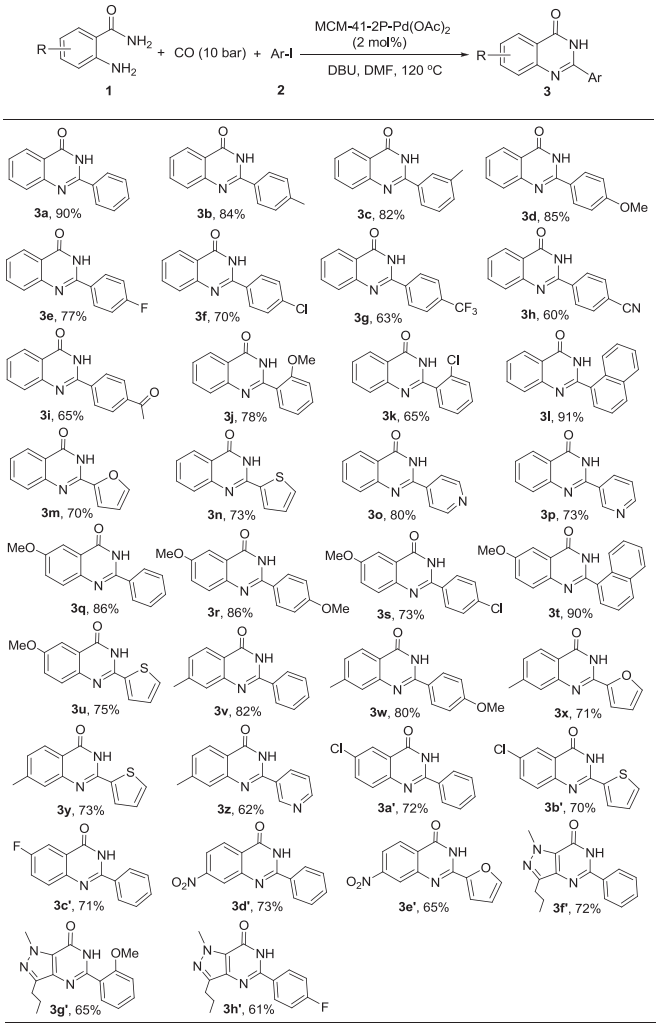

[a] Reaction conditions: **1** (1 mmol), **2** (1 mmol), DBU (2 mmol), MCM-41-2P-Pd(OAc)$_2$ (2 mol%) in DMF (2 mL) at 120 °C under 10 bar of CO for 20 h.
[b] Isolated yield.

removed by filtration from the solution at the reaction temperature (120 °C), and the filtrate was allowed to react further under identical reaction conditions. We found that, after this hot filtration, no increase in conversion of 2-aminobenzamide (**1a**) was observed. We also determined the palladium content in the filtrate by ICP-AES analysis, and no palladium was detected in the clear solution. These results exclude any contribution to the observed activity from the leached palladium species, indicating that MCM-41-2P-Pd(OAc)$_2$ was stable during the carbonylative annulation, and the observed catalysis was intrinsically heterogeneous.

2.4. Possible mechanism of heterogeneous Pd-catalyzed carbonylative annulation

A plausible reaction mechanism for this heterogeneous Pd-catalyzed carbonylative annulation is shown in Scheme 3. Firstly, MCM-41-2P-Pd(OAc)$_2$ is reduced by CO to MCM-41-2P-Pd(0). Oxidative addition of Ar-I (**2**) to MCM-41-2P-Pd(0) generates an MCM-41-anchored arylpalladium(II) complex **A**, which is followed by migratory insertion of carbon monoxide to produce an MCM-41-anchored acylpalladium(II) complex **B**. The reaction of intermediate **B** with 2-aminobenzamide (**1**) in the presence of DBU as base gives intermediate **C**, which undergoes reductive elimination to afford intermediate **D** and regenerate MCM-41-2P-Pd(0). Finally, intermediate **D** undergoes intramolecular condensation to furnish the desired quinazolinone (**3**). The intramolecular condensation of intermediate **D** to afford quinazolinones is responsible for the relatively high reaction temperature required.

2.5. Recycling of the catalyst

For the practical application of a heterogeneous precious metal catalyst system, its stability and reusability are important factors. The MCM-41-2P-Pd(OAc)$_2$ catalyst can be facilely separated and recovered by a simple filtration of the reaction mixture. We next examined the recycling of MCM-41-2P-Pd(OAc)$_2$ by using the carbonylative annulation reaction of 2-aminobenzamide (**1a**) with 1-iodonaphthalene (**2l**). After completion of the reaction, the catalyst was separated by simple filtration and washed with distilled water, DMF and diethyl ether. After being dried at 80 °C under vacuum for 1 h, the recovered palladium catalyst was used in the next run without further purification, and almost the same yield of **3l** was observed for eight consecutive cycles (91%, 90%, 91%, 90%, 89%, 90%, 89%, and 88%, respectively) as shown in Fig. 8. Besides, to examine palladium leaching of the heterogeneous catalyst, the palladium content of the recovered catalyst after eight consecutive runs was also determined by ICP-AES analysis and found to be 0.35 mmol/g, which is almost the same as that of the fresh one. The recycled MCM-41-2P-Pd(OAc)$_2$ was further characterized by X-ray photoelectron spectroscopy (XPS) (Fig. 7b). The observed binding energy values of 340.6 eV (Pd $3d^{3/2}$) and 335.4 eV (Pd $3d^{5/2}$) on the XPS spectrum of the recycled catalyst indicated that the state of palladium in the used catalyst was mainly Pd(0), which was in agreement with the proposed mechanism. In our opinion, there are two related factors that could explain the observed high catalytic activity and stability of MCM-41-2P-Pd(OAc)$_2$. First, the MCM-41 support has a regular pore diameter of ca. 5 nm and a specific surface area >700 m^2g^{-1} [38], which might give rise to efficient site isolation and the optimum dispersion of the active sites on the inner channel walls. The resulting nano-sized catalyst can serve as an efficient bridge and fill the gap between homogeneous and heterogeneous catalysts. In addition, the strong interaction between the bidentate phosphine ligand and the palladium centre immobilized on the MCM-41 resulted in the formation of a stable supported bidentate phosphine-palladium(II) complex, thereby greatly improving the reusability of the heterogeneous palladium catalyst.

3. Conclusions

In summary, we have developed a highly efficient heterogeneous palladium-catalyzed carbonylative annulation reaction of 2-aminobenzamides with aryl iodides under 10 bar of carbon monoxide leading to quinazolinones, which are commonly found in many bioactive molecules. This heterogeneous carbonylative annulation has many attractive features, such as: (1) the substrate scope is broad, and a wide range of 2-aminobenzamides and aryl iodides are allowed; (2) a variety of quinazolinone derivatives were obtained in mostly good to excellent yields; (3) the reaction is tolerant of a range of functional groups; (4) all of the products were purified by simple filtration or recrystallization, and no chromatography was needed; (5) this new palladium catalyst can easily be prepared *via* a simple procedure from commercially readily available reagents, and recovered by filtration of the reaction solution, and recycled up to eight times without significant loss of activity.

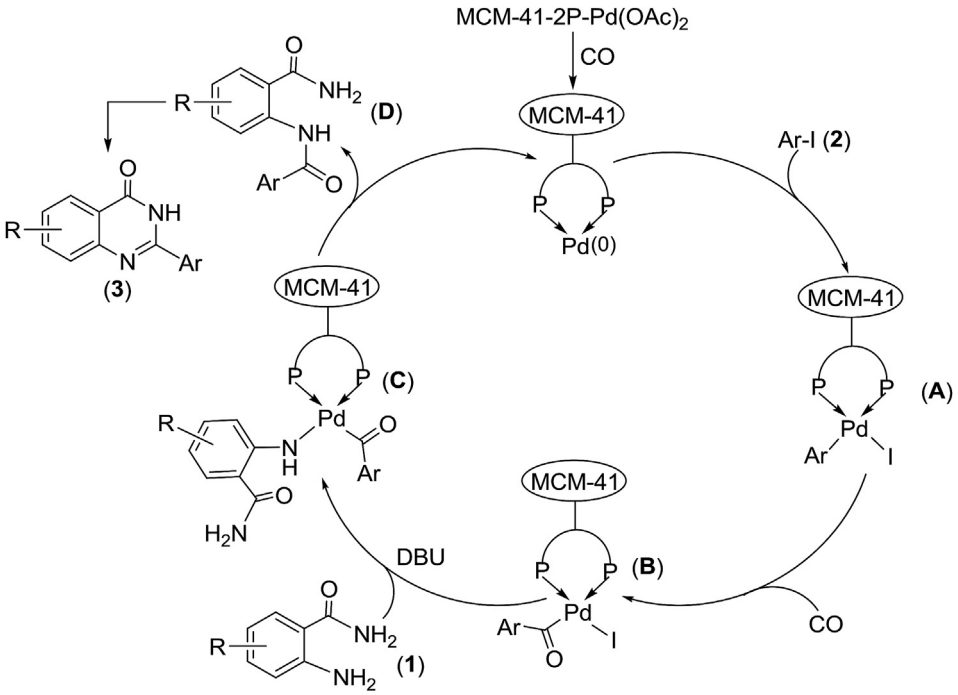

Scheme 3. Proposed catalytic cycle.

4. Experimental

4.1. General remarks

All reagents were obtained from commercial sources without further purification, and commercially available organic bases and solvents such as DIPEA (diisopropylethylamine), *n*-Bu_3N, DMAP (4-dimethylaminopyridine), DBU (1,8-diazabicyclo[5,4,0]undec-7-ene), DABCO (1,4-diazabicyclo [2,2,2]octane), dimethyl sulfoxide (DMSO), *N,N*-dimethylformamide (DMF), *N*-methyl-2-pyrrolidone (NMP), and 1,3-dimethyl-2-imidazolidone (DMI) were purified by vacuum distillation. Mesoporous material MCM-41 [38] and *N,N*-bis((diphenylphosphino)methyl)-3-(triethoxysilyl)propan-1-amine [54] were prepared according to literature methods. The products were purified by either washed with water, ethyl acetate and finally hexane or recrystallization from MeOH. All the products were characterized by comparison of their spectra and physical data with authentic samples. IR spectra were determined on a PerkinElmer 683 instrument. ^{1}H NMR spectra were recorded on a Bruker Avance 400 MHz spectrometer with TMS as an internal standard in DMSO-d_6 as solvent. ^{13}C NMR spectra (100 MHz) were recorded on a Bruker Avance 400 MHz spectrometer in DMSO-d_6 as solvent. HRMS spectra were recorded on a Q-Tof spectrometer with micromass MS software using electrospray ionization (ESI). Palladium content was determined with inductively coupled plasma atom emission Atomscan16 (ICP-AES, TJA Corporation). Microanalyses were measured by using a Yanaco MT-3 CHN microelemental analyzer. X-ray diffraction (XRD) measurements were carried out at room temperature using a Damx-rA (Rigaku) X-ray powder diffractmeter. X-ray energy dispersive spectroscopy (EDS) was performed using a microscope. Nitrogen adsorption/desorption isotherms were obtained using a Bel Japan Inc. Belsorp-HP at 77 K. Prior to gas adsorption measurements materials were degassed for 6 h at 423 K. The SEM analysis of the catalyst was recorded using a FESEM-TESCAN MIRA3. X-ray photoelectron spectra (XPS) were recorded on XSAM 800 (Kratos).

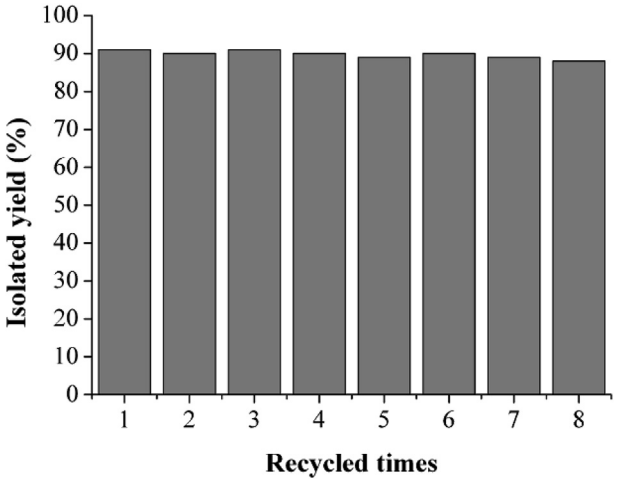

Fig. 8. Recycle of the MCM-41-2P-Pd(OAc)$_2$ complex.

4.2. Preparation of MCM-41-2P-Pd(OAc)$_2$ complex

N,N-Bis((diphenylphosphino)methyl)-3-(triethoxysilyl)propan-1-amine (0.927 g, 1.5 mmol) was added to a suspension of 2.0 g of the MCM-41 in 120 mL of dry toluene. The resulting mixture was stirred at 100 °C for 24 h under Ar. Then the solid was filtered, washed with $CHCl_3$ (20 mL), and dried in vacuum at 150 °C for 5 h. The dried white solid was then soaked in a solution of 2.5 g of Me_3SiCl in 100 mL of dry toluene at 25 °C under stirring for 24 h. The solid product was filtered, washed with acetone (3 × 20 mL), and dried in vacuum at 120 °C for 5 h to obtain 2.523 g of hybrid material MCM-41-2P. The phosphorus content was found to be 0.81 mmol/g by elemental analysis.

In a small Schlenk tube, 1.00 g of the above-functionalized MCM-41 (MCM-41-2P) was mixed with Pd(OAc)$_2$ (86 mg,

0.38 mmol) in 30 mL of dry acetone. The mixture was stirred at 60 °C for 72 h under an argon atmosphere. The solid product was filtered by suction, washed with acetone, distilled water and acetone successively and dried under vacuum at 80 °C for 5 h to give 1.03 g of a light yellow palladium(II) complex [MCM-41-2P-Pd(OAc)$_2$]. The phosphorus and palladium content were found to be 0.75 mmol/g and 0.36 mmol/g (3.83 wt%), respectively.

4.3. General procedure for the heterogeneous palladium-catalyzed carbonylative synthesis of quinazolinones

A 12 mL vial was charged with MCM-41-2P-Pd(OAc)$_2$ (2 mol%), 2-aminobenzamide (1 mmol), aryl iodide (1 mmol) (if solid) and a stirring bar. Then, DMF (2 mL), aryl iodide (1 mmol) (if liquid) and DBU (2 mmol) were injected by syringe under an argon atmosphere. The vial was placed in an alloy plate, which was transferred into a 300 mL Parr Instruments 4560 series autoclave under an argon atmosphere. After flushing the autoclave three times with CO, a pressure of 10 bar CO was fixed at ambient temperature. The autoclave was heated for 20 h at 120 °C. After completion of the reaction, the autoclave was cooled to room temperature and the pressure was released carefully. The reaction mixture was diluted with ethyl acetate (10 mL) and filtered. The palladium catalyst was washed with distilled water (2 × 5 mL) and acetone (2 × 5 mL), and reused in the next run. The filtrate was concentrated in vacuo and the pure product was isolated by either washed with water, ethyl acetate and finally hexane or recrystallization from MeOH.

4.3.1. 2-Phenylquinazolin-4(3H)-one (**3a**) [35]

White solid. IR (KBr): ν_{max}/cm^{-1} 3330, 3072, 1668, 1600, 1479, 1448, 1143, 946, 823, 763; ^{1}H NMR (400 MHz, DMSO-d_6): δ 12.55 (s, 1H), 8.21–8.15 (m, 3H), 7.85–7.80 (m, 1H), 7.74 (d, J = 8.0 Hz, 1H), 7.60–7.48 (m, 4H); ^{13}C NMR (100 MHz, DMSO-d_6): δ 162.7, 152.8, 149.2, 135.0, 133.2, 131.8, 129.0, 128.2, 128.0, 127.0, 126.3, 121.5.

4.3.2. 2-(4-Methylphenyl)quinazolin-4(3H)-one (**3b**) [55]

White solid. IR (KBr): ν_{max}/cm^{-1} 3332, 3070, 1666, 1601, 1477, 1449, 1145, 948, 823, 705; ^{1}H NMR (400 MHz, DMSO-d_6): δ 12.46 (s, 1H), 8.17 (d, J = 7.2 Hz, 1H), 8.12 (d, J = 8.0 Hz, 2H), 7.86–7.80 (m, 1H), 7.74 (d, J = 8.0 Hz, 1H), 7.52 (t, J = 7.6 Hz, 1H), 7.36 (d, J = 8.0 Hz, 2H), 2.40 (s, 3H); ^{13}C NMR (100 MHz, DMSO-d_6): δ 162.7, 152.7, 149.3, 141.9, 135.0, 130.4, 129.6, 128.1, 127.9, 126.8, 126.3, 121.4, 21.4.

4.3.3. 2-(3-Methylphenyl)quinazolin-4(3H)-one (**3c**)

White solid. IR (KBr): ν_{max}/cm^{-1} 3334, 3071, 1667, 1600, 1478, 1448, 1143, 946, 824, 765; ^{1}H NMR (400 MHz, DMSO-d_6): δ 12.47 (s, 1H), 8.16 (dd, J = 7.8, 1.0 Hz, 1H), 8.03 (s, 1H), 7.97 (d, J = 7.6 Hz, 1H), 7.86–7.81 (m, 1H), 7.75 (d, J = 7.6 Hz, 1H), 7.55–7.49 (m, 1H), 7.46–7.38 (m, 2H), 2.41 (s, 3H); ^{13}C NMR (100 MHz, DMSO-d_6): δ 162.7, 152.9, 149.2, 138.4, 135.1, 133.1, 132.5, 129.0, 128.7, 127.9, 127.1, 126.3, 125.3, 121.4, 21.4. HRMS calcd for $C_{15}H_{12}N_2O^+$ [M$^+$]: 236.0950, found 236.0961.

4.3.4. 2-(4-Methoxyphenyl)quinazolin-4(3H)-one (**3d**) [56]

White solid. IR (KBr): ν_{max}/cm^{-1} 3332, 3067, 1668, 1604, 1479, 1446, 1145, 944, 823, 763; ^{1}H NMR (400 MHz, DMSO-d_6): δ 12.41 (br, 1H), 8.21 (d, J = 8.8 Hz, 2H), 8.14 (dd, J = 8.0, 1.2 Hz, 1H), 7.84–7.79 (m, 1H), 7.71 (d, J = 7.6 Hz, 1H), 7.51–7.47 (m, 1H), 7.10 (d, J = 9.2 Hz, 2H), 3.86 (s, 3H); ^{13}C NMR (100 MHz, DMSO-d_6): δ 167.5, 167.1, 157.1, 154.2, 139.7, 134.7, 132.5, 131.3, 131.0, 130.0, 125.9, 119.2, 60.7.

4.3.5. 2-(4-Fluorophenyl)quinazolin-4(3H)-one (**3e**) [35]

White solid. IR (KBr): ν_{max}/cm^{-1} 3335, 3070, 1669, 1600, 1477, 1448, 1143, 946, 825, 708; ^{1}H NMR (400 MHz, DMSO-d_6): δ 12.56 (br, 1H), 8.28–8.23 (m, 2H), 8.16 (dd, J = 7.8, 1.0 Hz, 1H), 7.87–7.81 (m, 1H), 7.74 (d, J = 7.6 Hz, 1H), 7.58–7.50 (m, 1H), 7.39 (t, J = 9.0 Hz, 2H); ^{13}C NMR (100 MHz, DMSO-d_6): δ 164.5 (d, $^1J_{C\text{-}F}$ = 248.0 Hz), 162.7, 151.9, 135.1, 130.8 (d, $^3J_{C\text{-}F}$ = 9.0 Hz), 129.7, 129.1, 127.9, 127.1, 126.3, 121.3, 116.1 (d, $^2J_{C\text{-}F}$ = 21.8 Hz).

4.3.6. 2-(4-Chlorophenyl)quinazolin-4(3H)-one (**3f**) [55]

White solid. IR (KBr): ν_{max}/cm^{-1} 3330, 3072, 1665, 1603, 1476, 1450, 1146, 948, 823, 705; ^{1}H NMR (400 MHz, DMSO-d_6): δ 12.45 (br, 1H), 8.16 (dd, J = 8.0, 1.2 Hz, 1H), 8.10 (dd, J = 7.8, 1.0 Hz, 1H), 7.80–7.69 (m, 2H), 7.51–7.37 (m, 2H), 6.96–6.88 (m, 2H); ^{13}C NMR (100 MHz, DMSO-d_6): δ 167.4, 151.8, 149.1, 135.1, 132.2, 132.0, 130.1, 129.2, 129.1, 127.2, 126.3, 121.5.

4.3.7. 2-(4-Trifluoromethylphenyl)quinazolin-4(3H)-one (**3g**) [35]

White solid. IR (KBr): ν_{max}/cm^{-1} 3329, 3052, 1673, 1620, 1469, 1445, 1140, 956, 803; ^{1}H NMR (400 MHz, DMSO-d_6): δ 12.77 (br, 1H), 8.35 (d, J = 8.4 Hz, 2H), 8.18 (d, J = 8.0 Hz, 1H), 8.05 (d, J = 8.4 Hz, 2H), 7.88 (t, J = 7.6 Hz, 1H), 7.78 (d, J = 8.0 Hz, 1H), 7.57 (t, J = 7.4 Hz, 1H); ^{13}C NMR (100 MHz, DMSO-d_6): δ 162.6, 151.7, 148.9, 137.1, 135.2, 131.6 (q, $^2J_{C\text{-}F}$ = 31.9 Hz), 129.2, 128.1, 127.6, 126.4, 126.0 (q, $^3J_{C\text{-}F}$ = 3.2 Hz), 124.4 (q, $^1J_{C\text{-}F}$ = 270.5 Hz), 121.7.

4.3.8. 2-(4-Cyanophenyl)quinazolin-4(3H)-one (**3h**) [35]

White solid. IR (KBr): ν_{max}/cm^{-1} 3335, 3068, 2240, 1671, 1622, 1466, 1440, 1142, 958, 805; ^{1}H NMR (400 MHz, DMSO-d_6): δ 12.76 (br, 1H), 8.37 (d, J = 5.6 Hz, 2H), 8.18 (d, J = 6.4 Hz, 1H), 7.93 (d, J = 5.6 Hz, 2H), 7.92–7.78 (m, 2H), 7.58–7.56 (m, 1H); ^{13}C NMR (100 MHz, DMSO-d_6): δ 162.8, 150.7, 149.5, 138.7, 134.4, 132.3, 129.1, 127.8, 126.3, 125.8, 121.8, 116.8, 114.8.

4.3.9. 2-(4-Acetylphenyl)quinazolin-4(3H)-one (**3i**) [35]

White solid. IR (KBr): ν_{max}/cm^{-1} 3330, 3070, 1673, 1620, 1469, 1445, 1140, 956, 803; ^{1}H NMR (400 MHz, DMSO-d_6): δ 12.73 (s, 1H), 8.32 (d, J = 8.4 Hz, 2H), 8.18 (d, J = 7.6 Hz, 1H), 8.11 (d, J = 8.4 Hz, 2H), 7.88 (t, J = 7.8 Hz, 1H), 7.79 (d, J = 8.0 Hz, 1H), 7.57 (t, J = 7.6 Hz, 1H), 2.66 (s, 3H); ^{13}C NMR (100 MHz, DMSO-d_6): δ 198.2, 162.6, 152.0, 149.0, 139.1, 137.1, 135.2, 128.8, 128.6, 128.2, 127.5, 126.4, 121.6, 27.5.

4.3.10. 2-(2-Methoxyphenyl)quinazolin-4(3H)-one (**3j**)

White solid. IR (KBr): ν_{max}/cm^{-1} 3328, 3059, 2960, 1697, 1625, 1600, 1498, 1435, 1380, 1259, 1140, 956, 821; ^{1}H NMR (400 MHz, DMSO-d_6): δ 12.10 (s, 1H), 8.15 (dd, J = 8.0, 1.2 Hz, 1H), 7.84–7.80 (m, 1H), 7.73–7.69 (m, 2H), 7.56–7.51 (m, 2H), 7.20 (d, J = 8.4 Hz, 1H), 7.12–7.07 (m, 1H), 3.87 (s, 3H); ^{13}C NMR (100 MHz, DMSO-d_6): δ 161.7, 157.7, 152.8, 149.5, 134.9, 132.7, 130.9, 127.9, 127.0, 126.2, 123.1, 121.5, 120.9, 112.4, 56.3. HRMS calcd for $C_{15}H_{12}N_2O_2^+$ [M$^+$]: 252.0899, found 252.0896.

4.3.11. 2-(2-Chlorophenyl)quinazolin-4(3H)-one (**3k**)

Light yellow solid. IR (KBr): ν_{max}/cm^{-1} 3330, 3070, 1668, 1600, 1479, 1445, 1140, 946, 826, 725; ^{1}H NMR (400 MHz, DMSO-d_6): δ 12.53 (s, 1H), 8.21–8.16 (m, 2H), 7.85–7.82 (m, 1H), 7.77–7.73 (m, 1H), 7.59–7.53 (m, 4H); ^{13}C NMR (100 MHz, DMSO-d_6): δ 162.7, 152.8, 149.2, 135.1, 133.2, 131.9, 129.1, 128.2, 128.0, 127.1, 126.3, 121.5. HRMS calcd for $C_{14}H_9ClN_2O^+$ [M$^+$]: 256.0403, found 256.0412.

4.3.12. 2-(Naphthalen-1-yl)quinazolin-4(3H)-one (**3l**) [35]

Light yellow solid. IR (KBr): ν_{max}/cm^{-1} 3330, 3061, 1668, 1601, 1560, 1505, 1499, 1468, 1155, 944, 816, 724, 705; ^{1}H NMR (400 MHz, DMSO-d_6): δ 12.68 (s, 1H), 8.24 (dd, J = 7.6, 1.2 Hz, 1H), 8.13 (d, J = 8.0 Hz, 1H), 8.08 (d, J = 7.6 Hz, 1H), 8.04 (d, J = 8.0 Hz, 1H), 7.87–7.79 (m, 1H), 7.75 (d, J = 8.0 Hz, 1H), 7.66 (d, J = 7.6 Hz, 1H), 7.64 (d, J = 7.2 Hz, 1H), 7.62–7.56 (m, 3H); ^{13}C NMR (100 MHz,

DMSO-d_6): δ 162.4, 154.2, 149.2, 135.0, 133.6, 132.2, 130.9, 130.8, 128.8, 128.2, 127.9, 127.5, 127.3, 126.8, 126.3, 125.7, 125.5, 121.7.

*4.3.13. 2-(Furane-2-yl)quinazolin-4(3H)-one (**3m**) [56]*

Light yellow solid. IR (KBr): ν_{max}/cm^{-1} 3335, 3070, 1668, 1600, 1560, 1448, 1155, 944, 823, 763, 705; ^{1}H NMR (400 MHz, DMSO-d_6): δ 12.52 (s, 1H), 8.13 (dd, J = 7.8, 1.0 Hz, 1H), 8.01 (d, J = 0.8 Hz, 1H), 7.79 (t, J = 7.2 Hz, 1H), 7.69 (d, J = 8.0 Hz, 1H), 7.64 (d, J = 3.2 Hz, 1H), 7.52–7.49 (m, 1H), 6.75 (dd, J = 3.4, 1.8 Hz, 1H); ^{13}C NMR (100 MHz, DMSO-d_6): δ 162.0, 149.2, 147.0, 146.6, 144.5, 135.1, 127.7, 126.9, 126.4, 121.6, 115.0, 113.0.

*4.3.14. 2-(Thiophen-2-yl)quinazolin-4(3H)-one (**3n**) [35]*

Light yellow solid. IR (KBr): ν_{max}/cm^{-1} 3330, 3071, 1667, 1601, 1479, 1448, 1157, 946, 821, 764, 708; ^{1}H NMR (400 MHz, DMSO-d_6): δ 12.68 (s, 1H), 8.26 (dd, J = 3.6, 0.8 Hz, 1H), 8.15 (dd, J = 8.0, 1.2 Hz, 1H), 7.88 (dd, J = 5.2, 0.8 Hz, 1H), 7.82–7.79 (m, 1H), 7.67 (d, J = 8.0 Hz, 1H), 7.53–7.49 (m, 1H), 7.27–7.24 (m, 1H); ^{13}C NMR (100 MHz, DMSO-d_6): δ 162.3, 149.1, 148.3, 137.9, 135.1, 132.6, 129.9, 128.9, 127.4, 126.8, 126.5, 121.4.

*4.3.15. 2-(Pyridin-4-yl)quinazolin-4(3H)-one (**3o**) [35]*

Light yellow solid. IR (KBr): ν_{max}/cm^{-1} 3332, 3080, 2956, 1673, 1620, 1469, 1434, 1275, 1120, 821, 758; ^{1}H NMR (400 MHz, DMSO-d_6): δ 12.77 (s, 1H), 8.79 (dd, J = 4.8, 1.6 Hz, 2H), 8.19 (dd, J = 8.0, 1.2 Hz, 1H), 8.12 (dd, J = 4.8, 1.6 Hz, 2H), 7.91–7.86 (m, 1H), 7.80 (d, J = 8.0 Hz, 1H), 7.61–7.56 (m, 1H); ^{13}C NMR (100 MHz, DMSO-d_6): δ 162.6, 151.1, 150.7, 148.7, 140.5, 135.2, 128.2, 127.8, 126.4, 122.1, 122.0.

*4.3.16. 2-(Pyridin-3-yl)quinazolin-4(3H)-one (**3p**) [35]*

Light yellow solid. IR (KBr): ν_{max}/cm^{-1} 3330, 3070, 2958, 1671, 1624, 1469, 1445, 1275, 1140, 956, 803; ^{1}H NMR (400 MHz, DMSO-d_6): δ 12.73 (s, 1H), 9.30 (d, J = 2.0 Hz, 1H), 8.76 (dd, J = 4.6, 1.4 Hz, 1H), 8.52–8.49 (m, 1H), 8.18 (dd, J = 7.8, 1.0 Hz, 1H), 7.87–7.84 (m, 1H), 7.78 (d, J = 8.0 Hz, 1H), 7.61–7.54 (m, 2H); ^{13}C NMR (100 MHz, DMSO-d_6): δ 162.6, 152.3, 151.2, 149.2, 148.9, 135.9, 135.2, 129.2, 128.0, 127.4, 126.3, 124.0, 121.6.

*4.3.17. 6-Methoxy-2-phenylquinazolin-4(3H)-one (**3q**) [57]*

White solid. IR (KBr): ν_{max}/cm^{-1} 3332, 3071, 1668, 1600, 1479, 1448, 1145, 944, 823, 763; ^{1}H NMR (400 MHz, DMSO-d_6): δ 12.51 (s, 1H), 8.16 (dd, J = 7.8, 1.4 Hz, 2H), 7.69 (d, J = 8.8 Hz, 1H), 7.58–7.51 (m, 4H), 7.43 (dd, J = 9.0, 3.0 Hz, 1H), 3.89 (s, 3H); ^{13}C NMR (100 MHz, DMSO-d_6): δ 162.5, 158.2, 150.6, 143.7, 133.3, 131.5, 129.7, 129.0, 128.0, 124.6, 122.2, 106.3, 56.1.

*4.3.18. 6-Methoxy-2-(4-Methoxyphenyl)quinazolin-4(3H)-one (**3r**)*

White solid. IR (KBr): ν_{max}/cm^{-1} 3334, 3073, 1667, 1601, 1478, 1449, 1147, 942, 825, 765; ^{1}H NMR (400 MHz, DMSO-d_6): δ 12.38 (br, 1H), 8.16 (d, J = 8.8 Hz, 2H), 7.66 (d, J = 8.8 Hz, 1H), 7.53 (d, J = 3.2 Hz, 1H), 7.43 (dd, J = 8.8, 3.2 Hz, 1H), 7.08 (d, J = 8.8 Hz, 2H), 3.89 (s, 3H), 3.85 (s, 3H); ^{13}C NMR (100 MHz, DMSO-d_6): δ 162.6, 162.1, 157.9, 150.3, 143.7, 129.6, 129.3, 125.3, 124.5, 121.9, 114.4, 106.4, 56.1, 55.9. HRMS calcd for $C_{16}H_{14}N_2O_3^+$ [M$^+$]: 282.1004, found 282.1005.

*4.3.19. 6-Methoxy-2-(4-chlorophenyl)quinazolin-4(3H)-one (**3s**)*

White solid. IR (KBr): ν_{max}/cm^{-1} 3331, 3070, 1666, 1600, 1479, 1445, 1143, 946, 820, 705; ^{1}H NMR (400 MHz, DMSO-d_6): δ 12.57 (br, 1H), 8.18 (d, J = 8.4 Hz, 2H), 7.70 (d, J = 8.8 Hz, 1H), 7.61 (d, J = 8.4 Hz, 2H), 7.54 (d, J = 3.2 Hz, 1H), 7.45 (dd, J = 8.8, 2.8 Hz, 1H), 3.90 (s, 3H); ^{13}C NMR (100 MHz, DMSO-d_6): δ 162.4, 158.4, 149.6, 143.5, 136.4, 132.1, 129.8, 129.7, 129.1, 124.6, 122.3, 106.4, 56.1. HRMS calcd for $C_{15}H_{11}ClN_2O_2^+$ [M$^+$]: 286.0509, found 286.0504.

*4.3.20. 6-Methoxy-2-(naphthalen-1-yl)quinazolin-4(3H)-one (**3t**)*

Yellow solid. IR (KBr): ν_{max}/cm^{-1} 3330, 3061, 1668, 1601, 1560, 1499, 1468, 1155, 944, 816, 724, 705; ^{1}H NMR (400 MHz, DMSO-d_6): δ 12.64 (s, 1H), 8.19–8.16 (m, 1H), 8.11 (d, J = 8.4 Hz, 1H), 8.06–8.03 (m, 1H), 7.79 (dd, J = 7.2, 0.8 Hz, 1H), 7.70 (d, J = 8.8 Hz, 1H), 7.67–7.56 (m, 4H), 7.48 (dd, J = 8.8, 3.2 Hz, 1H), 3.93 (s, 3H); ^{13}C NMR (100 MHz, DMSO-d_6): δ 162.2, 158.4, 151.8, 143.7, 133.6, 132.2, 130.8, 130.7, 129.7, 128.8, 128.1, 127.5, 126.8, 125.7, 125.5, 124.4, 122.5, 106.4, 56.2. HRMS calcd for $C_{19}H_{14}N_2O_2^+$ [M$^+$]: 302.1055, found 302.1047.

*4.3.21. 6-Methoxy-2-(thiophen-2-yl)quinazolin-4(3H)-one (**3u**) [22]*

Pale yellow solid. IR (KBr): ν_{max}/cm^{-1} 3332, 3070, 1668, 1600, 1479, 1448, 1155, 944, 823, 764, 712; ^{1}H NMR (400 MHz, DMSO-d_6): δ 12.63 (br, 1H), 8.21–8.19 (m, 1H), 7.83 (d, J = 4.8 Hz, 1H), 7.62 (d, J = 8.8 Hz, 1H), 7.54 (d, J = 2.8 Hz, 1H), 7.41 (dd, J = 9.0, 3.0 Hz, 1H), 7.23 (dd, J = 5.0, 3.8 Hz, 1H), 3.89 (s, 3H); ^{13}C NMR (100 MHz, DMSO-d_6): δ 162.0, 158.1, 146.3, 143.5, 138.0, 131.9, 129.2, 128.8, 124.5, 122.2, 106.7, 56.1.

*4.3.22. 7-Methyl-2-phenylquinazolin-4(3H)-one (**3v**) [57]*

White solid. IR (KBr): ν_{max}/cm^{-1} 3330, 3071, 1665, 1603, 1475, 1447, 1143, 946, 823, 765; ^{1}H NMR (400 MHz, DMSO-d_6) δ 12.44 (br, 1H), 8.18–8.16 (m, 2H), 8.03 (d, J = 8.0 Hz, 1H), 7.60–7.51 (m, 4H), 7.32 (d, J = 8.0 Hz, 1H), 2.45 (s, 3H); ^{13}C NMR (100 MHz, DMSO-d_6): δ 162.6, 152.8, 149.3, 145.5, 133.3, 131.8, 129.0, 128.4, 128.2, 127.6, 126.2, 119.0, 21.8.

*4.3.23. 7-Methyl-2-(4-methoxyphenyl)quinazolin-4(3H)-one (**3w**) [22]*

Light yellow solid. IR (KBr): ν_{max}/cm^{-1} 3332, 3071, 1666, 1601, 1479, 1449, 1145, 944, 823, 763; ^{1}H NMR (400 MHz, DMSO-d_6): δ 12.29 (s, 1H), 8.17 (d, J = 8.8 Hz, 2H), 8.00 (d, J = 8.0 Hz, 1H), 7.49 (s, 1H), 7.28 (d, J = 8.4 Hz, 1H), 7.07 (d, J = 8.8 Hz, 2H), 3.84 (s, 3H), 2.44 (s, 3H); ^{13}C NMR (100 MHz, DMSO-d_6): δ 162.6, 162.3, 152.3, 149.5, 145.4, 129.8, 128.0, 127.4, 126.1, 125.4, 118.8, 114.4, 55.9, 21.8.

*4.3.24. 7-Methyl-2-(furane-2-yl)quinazolin-4(3H)-one (**3x**) [22]*

Light yellow solid. IR (KBr): ν_{max}/cm^{-1} 3335, 3073, 1668, 1602, 1560, 1479, 1447, 1155, 944, 823, 763, 705.^{1}H NMR (400 MHz, DMSO-d_6): δ 12.39 (s, 1H), 8.00–7.97 (m, 2H), 7.60 (d, J = 3.6 Hz, 1H), 7.47 (s, 1H), 7.28 (d, J = 8.0 Hz, 1H), 6.73 (dd, J = 3.6 Hz, 1.6 Hz, 1H), 2.43 (s, 3H); ^{13}C NMR (100 MHz, DMSO-d_6): δ 161.9, 149.2, 146.9, 146.6, 145.5, 144.5, 128.3, 127.4, 126.2, 119.2, 114.8, 112.9, 21.8.

*4.3.25. 7-Methyl-2-(thiophen-2-yl)quinazolin-4(3H)-one (**3y**) [22]*

Light yellow solid. IR (KBr): ν_{max}/cm^{-1} 3330, 3070, 1669, 1600, 1478, 1448, 1143, 946, 823, 706; ^{1}H NMR (400 MHz, DMSO-d_6): δ 12.54 (s, 1H), 8.22 (d, J = 3.2 Hz, 1H), 8.01 (d, J = 8.0 Hz, 1H), 7.85 (d, J = 4.8 Hz, 1H), 7.47 (s, 1H), 7.31 (d, J = 8.0 Hz, 1H), 7.24 (dd, J = 4.8, 4.0 Hz, 1H), 2.46 (s, 3H); ^{13}C NMR (100 MHz, DMSO-d_6): δ 162.1, 149.2, 148.3, 145.7, 138.0, 132.5, 129.7, 128.9, 128.2, 127.1, 126.3, 118.9, 21.8.

*4.3.26. 7-Methyl-2-(pyridin-3-yl)quinazolin-4(3H)-one (**3z**)*

Light yellow solid. IR (KBr): ν_{max}/cm^{-1} 3331, 3070, 2958, 1675, 1625, 1600, 1469, 1445, 1380, 1140, 956, 803; ^{1}H NMR (400 MHz, DMSO-d_6): δ 12.59 (s, 1H), 9.28 (d, J = 2.0 Hz, 1H), 8.74 (dd, J = 4.8, 1.6 Hz, 1H), 8.48–8.45 (m, 1H), 8.02 (d, J = 8.0 Hz, 1H), 7.58–7.53 (m, 2H), 7.33 (dd, J = 8.0, 1.2 Hz, 1H), 2.45 (s, 3H); ^{13}C NMR (100 MHz, DMSO-d_6): δ 162.4, 152.2, 151.1, 149.2, 149.1, 145.6, 135.7, 129.2, 128.8, 127.6, 126.2, 123.9, 119.2, 21.8. HRMS calcd for $C_{14}H_{11}N_3O^+$ [M$^+$]: 237.0902, found 237.0911.

*4.3.27. 6-Chloro-2-phenylquinazolin-4(3H)-one (**3a'**) [58]*

White solid. IR (KBr): ν_{max}/cm^{-1} 3331, 3073, 1666, 1601, 1479, 1449, 1143, 946, 823, 705; ^{1}H NMR (400 MHz, DMSO-d_6): δ 12.69 (br, 1H), 8.16 (d, J = 7.2 Hz, 2H), 8.08 (d, J = 2.0 Hz, 1H), 7.87–7.83 (m, 1H), 7.76 (d, J = 8.4 Hz, 1H), 7.63–7.53 (m, 3H); ^{13}C NMR (100 MHz, DMSO-d_6): δ 161.8, 153.4, 147.9, 135.2, 132.9, 132.1, 131.3, 130.1, 129.1, 128.3, 125.3, 122.7.

*4.3.28. 6-Chloro-2-(thiophen-2-yl)quinazolin-4(3H)-one (**3b'**) [58]*

White solid. IR (KBr): ν_{max}/cm^{-1} 3332, 3072, 1669, 1600, 1477, 1448, 1145, 947, 823, 706; ^{1}H NMR (400 MHz, DMSO-d_6): δ 12.76 (s, 1H), 8.21 (d, J = 3.2 Hz, 1H), 8.01 (d, J = 2.0 Hz, 1H), 7.87 (d, J = 4.8 Hz, 1H), 7.77 (dd, J = 8.8, 2.4 Hz, 1H), 7.63 (d, J = 8.4 Hz, 1H), 7.23 (t, J = 4.4 Hz, 1H); ^{13}C NMR (100 MHz, DMSO-d_6): δ 161.3, 148.7, 147.9, 137.5, 135.1, 132.9, 130.9, 130.2, 129.6, 129.0, 125.5, 122.5.

*4.3.29. 6-Fluoro-2-phenylquinazolin-4(3H)-one (**3c'**)*

White solid. IR (KBr): ν_{max}/cm^{-1} 3331, 3070, 1667, 1602, 1478, 1449, 1143, 946, 825, 708; ^{1}H NMR (400 MHz, DMSO-d_6): δ 12.63 (br, 1H), 8.16 (d, J = 7.2 Hz, 2H), 7.83–7.77 (m, 2H), 7.74–7.68 (m, 1H), 7.60–7.52 (m, 3H); ^{13}C NMR (100 MHz, DMSO-d_6): δ 162.1, 160.5 (d, $^1J_{C\text{-}F}$ = 243.9 Hz), 152.4, 146.1, 133.0, 131.9, 130.7, 129.1, 128.2, 123.5 (d, $^2J_{C\text{-}F}$ = 23.9 Hz), 122.6 (d, $^3J_{C\text{-}F}$ = 8.3 Hz), 110.9 (d, $^2J_{C\text{-}F}$ = 23.2 Hz). HRMS calcd for $C_{14}H_9FN_2O^+$ [M$^+$]: 240.0699, found 240.0697.

*4.3.30. 7-Nitro-2-phenylquinazolin-4(3H)-one (**3d'**) [22]*

Yellow solid. IR (KBr): ν_{max}/cm^{-1} 3330, 3070, 1668, 1600, 1518, 1448, 1352, 1143, 946, 823, 705; ^{1}H NMR (400 MHz, DMSO-d_6): δ 12.91 (br, 1H), 8.45 (d, J = 2.4 Hz, 1H), 8.37 (d, J = 8.4 Hz, 1H), 8.25–8.20 (m, 3H), 7.65–7.56 (m, 3H); ^{13}C NMR (100 MHz, DMSO-d_6): δ 161.9, 155.1, 151.8, 149.6, 132.6, 132.5, 129.2, 128.6, 128.5, 125.8, 122.8, 120.5.

*4.3.31. 7-Nitro-2-(furane-2-yl)quinazolin-4(3H)-one (**3e'**)*

Yellow solid. IR (KBr): ν_{max}/cm^{-1} 3335, 3070, 1668, 1601, 1520, 1479, 1448, 1342, 944, 823, 763, 705; ^{1}H NMR (400 MHz, DMSO-d_6): δ 12.43 (s, 1H), 9.29 (d, J = 1.6 Hz, 1H), 9.24 (d, J = 2.4 Hz, 1H), 8.45 (d, J = 8.8 Hz, 1H), 8.39–8.33 (m, 2H), 7.44 (d, J = 8.8 Hz, 1H); ^{13}C NMR (100 MHz, DMSO-d_6): δ 160.1, 151.0, 142.8, 142.2, 134.6, 130.2, 126.0, 123.4, 120.9, 119.5, 117.7, 117.1. HRMS calcd for $C_{12}H_7N_3O_4^+$ [M$^+$]: 257.0437, found 257.0429.

*4.3.32. 1-Methyl-5-phenyl-3-propyl-1H-pyrazolo[4,3-d]pyrimidin-7(6H)-one (**3f'**) [35]*

White solid. IR (KBr): ν_{max}/cm^{-1} 3268, 3171, 2960, 2872, 1697, 1561, 1498, 1434, 1390, 1259, 1238, 823, 758; ^{1}H NMR (400 MHz, DMSO-d_6): δ 12.41 (s, 1H), 8.08–8.05 (m, 2H), 7.73–7.68 (m, 1H), 7.58–7.50 (m, 2H), 4.16 (s, 3H), 2.79 (t, J = 7.4 Hz, 2H), 1.80–1.75 (m, 2H), 0.96 (t, J = 7.2 Hz, 3H); ^{13}C NMR (100 MHz, DMSO-d_6): δ 154.4, 151.5, 144.3, 135.9, 133.2, 128.3, 124.9, 119.5, 118.0, 38.4, 27.7, 22.1, 14.3.

*4.3.33. 1-Methyl-5-(2-methoxyphenyl)-3-propyl-1H-pyrazolo[4,3-d]pyrimidin-7(6H)-one (**3g'**)*

White solid. IR (KBr): ν_{max}/cm^{-1} 3280, 3170, 2960, 1687, 1560, 1435, 1380, 1263, 1211, 928, 823; ^{1}H NMR (400 MHz, DMSO-d_6): δ 12.32 (br, 1H), 8.13 (dd, J = 8.0, 1.2 Hz, 1H), 7.40 (t, J = 7.6 Hz, 1H), 6.99 (d, J = 8.0 Hz, 1H), 6.95 (t, J = 7.6 Hz, 1H), 4.16 (s, 3H), 3.82 (s, 3H), 2.80 (t, J = 7.4 Hz, 2H), 1.78–1.72 (m, 2H), 0.95 (t, J = 7.4 Hz, 3H); ^{13}C NMR (100 MHz, DMSO-d_6): δ 167.1, 161.1, 155.1, 147.6, 134.2, 133.4, 132.4, 129.0, 128.1, 128.0, 116.6, 60.2, 39.4, 27.9, 21.7, 14.3. HRMS calcd for $C_{16}H_{18}N_4O_2^+$ [M$^+$]: 298.1430, found 298.1435.

*4.3.34. 1-Methyl-5-(4-fluorophenyl)-3-propyl-1H-pyrazolo[4,3-d]pyrimidin-7(6H)-one (**3h'**)*

White solid. IR (KBr): ν_{max}/cm^{-1} 3264, 3064, 2933, 1675, 1575, 1421, 1311, 1145, 947, 836, 769; ^{1}H NMR (400 MHz, DMSO-d_6): δ 12.44 (br, 1H), 8.15–8.11 (m, 2H), 7.36 (t, J = 8.8 Hz, 2H), 4.15 (s, 3H), 2.78 (t, J = 7.4 Hz, 2H), 1.80–1.74 (m, 2H), 0.95 (t, J = 7.4 Hz, 3H); ^{13}C NMR (100 MHz, DMSO-d_6): δ 164.0 (d, $^1J_{C\text{-}F}$ = 254.5 Hz), 155.1, 149.7, 145.4, 138.3, 130.5 (d, $^3J_{C\text{-}F}$ = 8.8 Hz), 129.9, 124.8, 116.0 (d, $^2J_{C\text{-}F}$ = 21.8 Hz), 38.3, 27.6, 22.1, 14.3. HRMS calcd for $C_{15}H_{15}FN_4O^+$ [M$^+$]: 286.1230, found 286.1227.

Acknowledgements

We thank the National Natural Science Foundation of China (No. 21462021) and Key Laboratory of Functional Small Organic Molecule, Ministry of Education (No. KLFS-KF-201704) for financial support.

References

[1] J.P. Michael, Nat. Prod. Rep. 21 (2004) 650–668.
[2] S.B. Mhaske, N.P. Argade, Tetrahedron 62 (2006) 9787–9826.
[3] Y. Takase, T. Saeki, N. Watanabe, H. Adachi, S. Souda, I. Saito, J. Med. Chem. 37 (1994) 2106–2111.
[4] P.M. Chandrika, T. Yakaiah, A.R.R. Rao, B. Narsaiah, N.C. Reddy, V. Sridhar, J.V. Rao, Eur. J. Med. Chem. 43 (2008) 846–852.
[5] P.P. Kung, M.D. Casper, K.L. Cook, L. Wilson-Lingardo, L.M. Risen, T.A. Vickers, R. Ranken, L.B. Blyn, J.R. Wyatt, P.D. Cook, J. Med. Chem. 42 (1999) 4705–4713.
[6] J.-H. Chan, J.-S. Hong, L.F. Kuyper, D.P. Baccanari, S.S. Joyner, R.L. Tansik, C.M. Boytos, S.K. Rudolph, J. Med. Chem. 38 (1995) 3608–3616.
[7] H. Kikuchi, K. Yamamoto, S. Horoiwa, S. Hirai, R. Kasahara, N. Hariguchi, M. Matsumoto, Y. Oshima, J. Med. Chem. 49 (2006) 4698–4706.
[8] M.-H. Yen, J.-R. Sheu, I.-H. Peng, Y.-M. Lee, J.-W. Chern, J. Pharm. Pharmacol. 48 (1996) 90–95.
[9] J. Kunes, J. Bazant, M. Pour, K. Waisser, M. Slosarek, J. Janota, Farmaco 55 (2000) 725–729.
[10] K. Matsuno, J. Ushiki, T. Seishi, M. Ichimura, N.A. Giese, J.-C. Yu, S. Takahashi, S. Oda, Y. Nomoto, J. Med. Chem. 46 (2003) 4910–4925.
[11] A. Archana, V.K. Shrivastava, R. Chandra, A. Kumar, Indian J. Chem. 41B (2002) 2371–2375.
[12] A. Baba, N. Kawamura, H. Makino, Y. Ohta, S. Taketomi, T. Sohda, J. Med. Chem. 39 (1996) 5176–5182.
[13] B.Y. Daniel, W.G. Jason, L.S. Stephanie, V.P. Arely, T.C. Matthew, A.B. David, J. Dermatol. Sci. 42 (2006) 13–21.
[14] N. Malecki, P. Carato, G. Rigo, J.F. Goossens, R. Houssin, C. Bailly, J.P. Henichart, Bioorg. Med. Chem. 12 (2004) 641–647.
[15] Y. Feng, N. Tian, Y. Li, C. Jia, X. Li, L. Wang, X. Cui, Org. Lett. 19 (2017) 1658–1661.
[16] D.N. Garad, A.B. Viveki, S.B. Mhaske, J. Org. Chem. 82 (2017) 6366–6372.
[17] D.J. Connolly, D. Cusack, T.P. O'Sullivan, P.J. Guiry, Tetrahedron 61 (2005) 10153–10202.
[18] Y. Mitobe, S. Ito, T. Mizutani, T. Nagase, N. Sato, S. Tokita, Bioorg. Med. Chem. Lett 19 (2009) 4075–4078.
[19] L. Xu, Y. Jiang, D. Ma, Org. Lett. 14 (2012) 1150–1153.
[20] N.Y. Kim, C.-H. Cheon, Tetrahedron Lett. 55 (2014) 2340–2344.
[21] J.F. Liu, P. Ye, B. Zhang, G. Bi, K. Sargent, L. Yu, D. Yohannes, C.M. Baldino, J. Org. Chem. 70 (2005) 6339–6345.
[22] W. Xu, Y. Jin, H. Liu, Y. Jiang, H. Fu, Org. Lett. 13 (2011) 1274–1277.
[23] F. Li, L. Lu, P. Liu, Org. Lett. 18 (2016) 2580–2583.
[24] S.M.A.H. Siddiki, K. Kon, A.S. Touchy, K. Shimizu, Catal. Sci. Technol. 4 (2014) 1716–1721.
[25] H. Hikawa, Y. Ino, H. Suzuki, Y. Yokoyama, J. Org. Chem. 77 (2012) 7046–7051.
[26] Z. Zheng, H. Alper, Org. Lett. 10 (2008) 829–832.
[27] X. Jiang, T. Tang, J.-M. Wang, Z. Chen, Y.-M. Zhu, S.-J. Ji, J. Org. Chem. 79 (2014) 5082–5087.
[28] A. Schoenberg, I. Bartoletti, R.F. Heck, J. Am. Chem. Soc. 96 (1974) 7761–7764.
[29] X.F. Wu, H. Neumann, M. Beller, Chem. Soc. Rev. 40 (2011) 4986–5009.
[30] C.F.J. Barnard, Organometallics 27 (2008) 5402–5422.
[31] C. Shen, X.F. Wu, Chem. Eur J. 23 (2017) 2973–2987.
[32] X.F. Wu, H. Neumann, M. Beller, Chem. Rev. 113 (2013) 1–35.
[33] K. Natte, J. Chen, H. Li, H. Neumann, M. Beller, X.F. Wu, Chem. Eur J. 20 (2014) 14184–14188.
[34] H. Li, W. Li, A. Spannenberg, W. Baumann, H. Neumann, M. Beller, X.F. Wu, Chem. Eur J. 20 (2014) 8541–8544.
[35] G.M. Torres, J.S. Quesnel, D. Bijou, B.A. Arndtsen, J. Am. Chem. Soc. 138 (2016) 7315–7324.
[36] X.F. Wu, L. He, H. Neumann, M. Beller, Chem. Eur J. 19 (2013) 12635–12638.
[37] A. Molnar, Chem. Rev. 111 (2011) 2251–2320.
[38] C.T. Kresge, M.E. Leonowicz, W.J. Roth, J.C. Vartuli, J.S. Beck, Nature 359 (1992)

710–712.
[39] A. Corma, Top. Catal. 4 (1997) 249–260.
[40] R.M. Martin-Aranda, J. Cejka, Top. Catal. 53 (2010) 141–153.
[41] P.C. Mehnert, D.W. Weaver, J.Y. Ying, J. Am. Chem. Soc. 120 (1998) 12289–12296.
[42] K. Mukhopadhyay, B.R. Sarkar, R.V. Chaudhari, J. Am. Chem. Soc. 124 (2002) 9692–9693.
[43] M. Cai, J. Peng, W. Hao, G. Ding, Green Chem. 13 (2011) 190–196.
[44] F. Havasi, A. Ghorbani-Choghamarani, F. Nikpour, New J. Chem. 39 (2015) 6504–6512.
[45] Y. Yang, R.M. Rioux, Chem. Commun. 47 (2011) 6557–6559.
[46] M. Jia, A. Seifert, W.R. Thiel, Chem. Mater. 15 (2003) 2174–2180.
[47] A. Corma, E. Gutierrez-Puebla, M. Iglesias, A. Monge, S. Perez-Ferreras, F. Sanchez, Adv. Synth. Catal. 348 (2006) 1899–1907.
[48] G. Villaverde, A. Corma, M. Iglesias, F. Sanchez, ACS Catal. 2 (2012) 399–406.
[49] W. Yang, R. Zhang, F. Yi, M. Cai, J. Org. Chem. 82 (2017) 5204–5211.
[50] H. Zhao, W. He, R. Yao, M. Cai, Adv. Synth. Catal. 356 (2014) 3092–3098.
[51] M. Cai, R. Yao, L. Chen, H. Zhao, J. Mol. Catal. Chem. 395 (2014) 349–354.
[52] H. Zhao, W. He, L. Wei, M. Cai, Catal. Sci. Technol. 6 (2016) 1488–1495.
[53] H.E.B. Lempers, R.A. Sheldon, J. Catal. 175 (1998) 62–69.
[54] T. Posset, J. Guenther, J. Pope, T. Oeser, J. Blumel, Chem. Commun. 47 (2011) 2059–2061.
[55] X. Zhang, D. Ye, H. Sun, D. Guo, J. Wang, H. Huang, X. Zhang, H. Jiang, H. Liu, Green Chem. 11 (2009) 1881–1887.
[56] J. Chen, D. Wu, F. He, M. Liu, H. Wu, J. Ding, W. Su, Tetrahedron Lett. 49 (2008) 3814–3818.
[57] O.K. Ahmad, M.D. Hill, M. Movassaghi, J. Org. Chem. 74 (2009) 8460–8463.
[58] X. Liu, H. Fu, Y. Jiang, Y. Zhao, Angew. Chem. 121 (2009) 354–358.